www.serd.ait.ac.th/reric

Determination of Optimum Angles for Solar Energy Conversions into Heat and Electricity

Anand M. Sharan*[1]

Abstract – *In this paper, the optimum energy conversion condition of a stationary panel is calculated. These calculations are done for 180 days at different latitudes. Various angular orientations of the sun's rays on the earth are considered. On a given day, the incident energy flux of the sun is resolved into three components, and the conversion efficiency is based on the flux normal for the panels. The efficiency of the conversion of the incident energy is measured with respect to a solar tracking process. The numbers of days in a given year are divided into two groups – between the winter solstice and the spring equinox and between the spring equinox and the summer solstice. The results show the existence of two maxima with one for each of the two periods. By setting the panels at each of these maxima, very significant improvement in energy conversion can be achieved.*

Keywords – Alternate energy, experimental measurement of efficiency, photovoltaic systems solar energy.

1. INTRODUCTION

In today's world, there is great importance being attached to burning less fossil fuels whose combustion causes increase in CO_2 levels in the atmosphere which in turn causes global warming. In addition, experts are predicting that we will soon see a shortage in oil supplies due to the increased demand for oil in both industrialized and newly industrializing countries [1]. Added to this, the depletion of forests is also leading to increased global warming. Given these factors, it is ever more imperative to use alternate energy sources and improve efficiencies of the presently used energy conversion systems.

Solar energy provides us with an alternative where there is no pollution of the environment and whose use decreases the rate of depletion of energy reserves. The main uses of solar energy have been in converting this energy into heat and electricity. In the first case, the sun's rays are used directly for, heating homes or water heating where the sun's rays are incident on a panel containing circulating water in tubes. In the second case, one generates electricity using photovoltaic panels. In the majority of cases, these panels are held stationary at an angle from the horizontal plane facing towards a southerly direction. This angle is not changed irrespective of seasons.

There have been different approaches to harnessing solar energy. In one approach [2]–[5], efforts have been made to enhance the energy conversion at the solar cell level. This leads to energy conversion from approximately 12% to 15% of the incident energy, as far as the conversion of the sun's energy into electricity is concerned. The second approach uses improved control in power generation [6]–[15]. In this approach, the electrical parameters involved in the power generation are altered through the control process which includes the use of microprocessors in some cases. One can also refer to some other relevant references [16]–[22]. The availability of solar energy (daily totals and hourly fluxes) between the 25 ^{0} N, and 25 ^{0} S of the equator (in the tropical areas with monsoon) is discussed in [23].

In a tracking process, the solar panels are mounted on a mechanism which is driven by a motor. The two necessary angles are adjusted in such a way that the sun's ray is always normal for the panels. Even though the tracking process yields the maximum possible energy conversion as compared to other processes, the majority of the energy conversion units are not designed to do the tracking. In such cases, the receiving surface is held at a constant horizontal angle year round, irrespective of the seasons.

The objective of this work is to show that such an arrangement of holding panels at an arbitrary angle from the horizontal is not appropriate. In this paper determination is made of optimum angles in each of the two periods; between (a) the winter solstice and spring equinox and (b) between spring equinox and summer solstice.

2. LIMITATIONS OF THIS WORK

This work does not deal with issues involving:

1. The design of receivers which is dependent upon material properties such as absorptivity or reflectivity. Appendix A of this paper has a brief discussion on energy losses which take place after the sunrays are incident on such panels.

2. Absorption of energy by (a) gases or (b) water vapor in the atmosphere, or (c) Raleigh scattering by molecules in atmosphere or dust or (e) Mie scattering.

This work deals with only the direct beam radiation incident on the solar panel after it has gone through the atmospheric losses at the location where the energy is being converted.

3. The work does not take into account the wobbly motion of the earth which is an extremely slow varying cause and whose magnitude is extremely small as compared to the amounts of energy under discussion here.

This paper makes an attempt to maximize the solar energy output given the incident solar radiation after the sun's rays have traveled through the atmosphere. Needless to say, the incident radiation itself varies due to seasons

* Faculty of Engineering Memorial University St. John's, NL A1B 3X5, Canada.

[1] Corresponding author;
Tel: 709-737-8930, Fax 709-737-4042.
E-mail: asharan@mun.ca.

and local atmospheric conditions. The results here clearly show that - given the choice between tracking and stationary systems, one always obtains far higher efficiency in the tracking process.

3. THEORETICAL CONSIDERATIONS

Figure 1 shows the sun's rays incident on a horizontal plane, and the incident angle of the rays are indicated by angles α_s and α in the horizontal and vertical planes respectively.

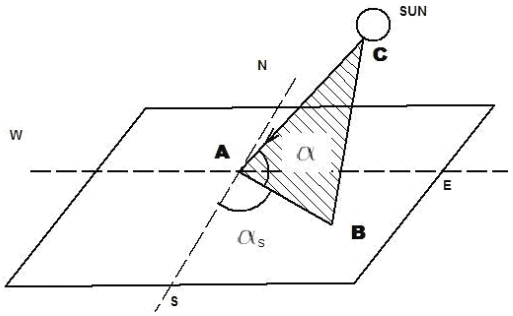

Fig. 1. Diagram showing the solar ray direction using two angles.

Suppose the distance AC is equal to R then the components in the X1, and Y1 directions will be (refer to Figure 2 for X1 and Y1 directions):

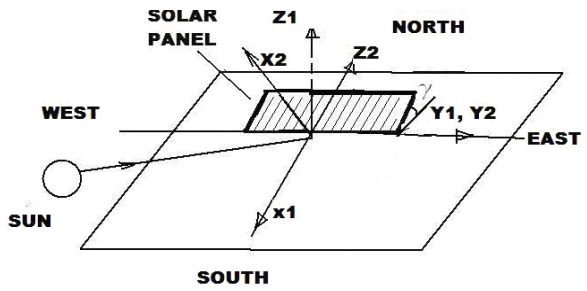

Fig. 2 Solar panel facing south and tilted at an angle equal to latitude of the place

X_B = R COS (α_s) or, by expressing the distance in a non dimensional manner, one can write:

$$(X_B / R) = \text{COS}\ (\alpha_s) \quad (1)$$

Similarly, one can write:

$$(Y_B / R) = \text{SIN}\ (\alpha_s)\ . \quad (2)$$

If the intensity of solar energy is I_0, then the three components in X1, Y1, and Z1 co-ordinates will be:

$$I_{X1} = - I_0 \cos(\alpha)\ \text{COS}\ (\alpha_s) \quad (3)$$

$$I_{Y1} = - I_0 \cos(\alpha)\ \text{SIN}\ (\alpha_s) \quad (4)$$

$$I_{Z1} = - I_0\ \text{SIN}\ (\alpha) \quad (5)$$

Let us represent the solar energy by a vector:

$$\{I\}^1 = \{\ I_{X1}\ ,\ I_{Y1}\ ,\ I_{Z1}\ \}^T .$$

In Figure 2, one can express the vector $\{I\}^2$ in terms of $\{I\}^1$ in the matrix form as [24]:

$$\{\ I\ \}^2 = [\ R\ (\ Y1, \eta\ )\ ]\ \ \{\ I\ \}^1 \quad (6)$$

3 x 1 3 x 3 3 x 1

In Figure 2, the X2 direction is perpendicular to the panel, and the angle:

$$(X2\text{- O -}X1)\ = \eta = (90 - \gamma) \quad (7)$$

Here, γ is the angle from the horizontal plane as shown in Figure 2. In Equation 6, [R (Y1, η)] is the rotation matrix to transform the vector $\{I\}^1$ from X1- Y1 - Z1 space to X2- Y2 - Z2 space about the Y1 axis. A (3 x 3) rotational transformation matrix about Y axis involving rotation angle θ is given by:

$$[T_y(\theta)] = \begin{bmatrix} \cos\theta & 0 & \sin\theta \\ 0 & 1 & 0 \\ -\sin\theta & 0 & \cos\theta \end{bmatrix} \quad (8)$$

In Equation 6, one needs to replace [R (Y1, η)] with [Ty (θ)] as per the equation:

$$[\text{Ty}\ (\theta)] = [\text{R}\ (\text{Y1}, \eta)]$$

i.e., one uses θ in place of η to transform a 3 x 1 incident energy vector $\{I_0\}$. It should be remembered that we are only interested in the negative component in the X2 direction i.e. I_{X2} should be negative. If this vector component is positive then there is no solar energy conversion by the panels due to the sun shining from behind the panels.

As far as the calculations of α_s and α are concerned, one can use the following formulas [25]–[27]:

$$\delta = 23.45 \sin\ \{(360 / 365)\ (284 + N)\} \quad (9)$$

where δ is the declination of the sun in degrees, and N is the day number, which is the number of the day in a year. For example, on January 1, N is equal to 1. The time of sunrise, $h_{sr,}$ in hour angle from the noon, is calculated by:

$$h_{sr} = \cos^{-1}\{-\ \tan(\delta)\ \tan(\gamma)\} \quad (10)$$

Denoting the instant of time in terms of hour angle from the noon as h_s, one can write:

$$\sin(\alpha)\ =\ \cos(\gamma)\cos(\delta)\cos(h_s) + \sin(\gamma)\sin(\delta) \quad (11)$$

and, by expressing the angles in degrees we get:

$$\alpha_s = \sin^{-1}\{\cos(\delta)\sin(h_s)/\cos(\alpha)\}$$

$$\text{if } \cos(h_s) > \{\tan(\delta)/\tan(\gamma)\} \quad (12)$$

or

$$\alpha_s = 180^o - \sin^{-1}\{\cos(\delta)\sin(h_s)/\cos(\alpha)\}$$

$$\text{if } \cos(h_s) < \{\tan(\delta)/\tan(\gamma)\} \quad (13)$$

4. RESULTS AND DISCUSSIONS

To study the effect of latitude on the conversion efficiencies of the stationary mounted solar panels, four different cities at different latitudes were selected. The cities and their latitudes are shown in Table 1. Singapore is near the equator; Patna is near the Tropic of Cancer; Helsinki near the Arctic Circle and Boulder Colorado in the United States has latitude between Patna and Helsinki.

Figures 3 and 4 show the position of the sun in the morning hours at Helsinki for N=1 (winter), and N=182 (summer) when the days are short and long, respectively.

Table 1. Latitudes of different cities.

City	Latitude (North)
Singapore	1^0 14’
Patna (Bihar, India)	25^0 37’
Boulder (Colorado, U. S. A.)	40^0 1’
Helsinki (Finland)	60^0 10’

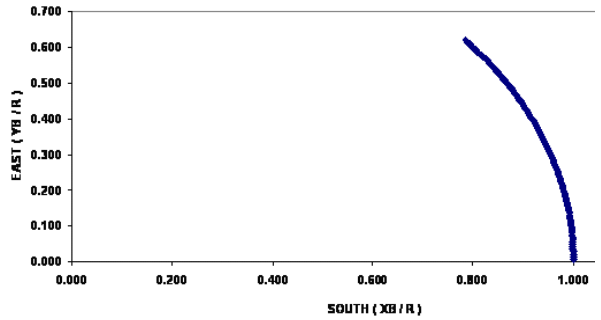

Fig. 3. Plot of sun’s trajectory at Helsinki, N=1.

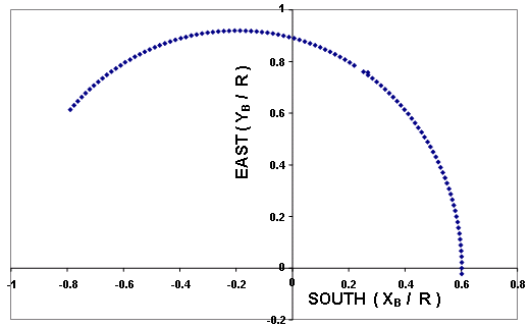

Fig. 4. Solar trajectory at Helsinki on N=182.

These figures were obtained by starting with Equation 8 and performing the calculations corresponding to Equations 9 to 12 followed by Equations 1 and 2; i.e., they are the plots of (Y_B/R) versus (X_B/R)–non dimensional distances.

In such plots, one can see the trajectory traversed by the trace of the sun on the horizontal plane. The morning sunshine period (between sunrise to noon) was divided into 100 intervals and calculations were made for each of the intervals. Due to the symmetry around noon, the afternoon values should be the same as the morning values.

For N=1 in Figure 3, the sun remains on the south side (refer to Figure 2) of the vertical plane containing the Y1 and Z1 axes.

Since this day is in the winter in the northern hemisphere, the days are much shorter at the high latitudes (e.g. Helsinki). The curvilinear length in Figure 3 is much shorter than in Figure 4. One can state this in another way where one can say that the span of angle α_s or α is greater for the two summer cases as compared to the winter cases. We will see later that this larger span in summer results in reduced conversion efficiency of these panels which are held at a fixed angle from the horizontal and face south in the northern hemisphere. This increased span results from the increase in the latitude of a place. The difference in the span between the summer and the winter is reduced near the equator like in the case of Singapore.

The fact that the efficiency of the panel is reduced because it faces only in one direction which is south all the year round. In summer in Singapore, the sun rises in the north-east and sets in the north-west without crossing the east -west line i.e. without going to the south at all. In the winter, the sun rises in the south-east and sets in south-west in both the places without crossing the east west line. Thus, the efficiency is higher in the winter as compared to the summer. In order to overcome this problem, it was decided that an optimum angle for a six month period needed to be found. Therefore, the calculations were performed for angles between -85 to 85 degrees at a one degree interval for the four cities of the study. Figure 5 shows the panels at the positive and negative values of their orientation from the horizontal plane.

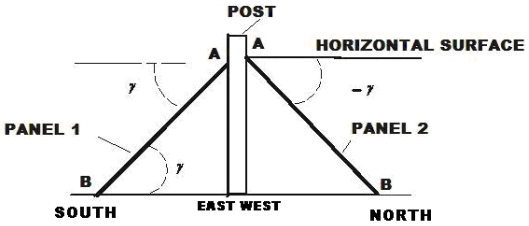

Fig. 5. inclination of panels from horizontal surface (panel number 2 at negative angle).

Figure 6 shows the conversion efficiency as a function of an angle at which the panel is held from the horizontal plane represented by γ in Figure 2.

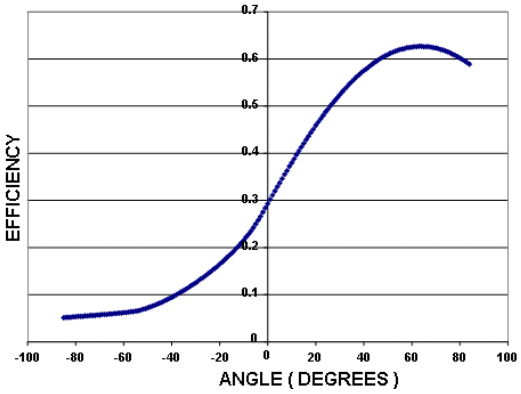

Fig. 6. Efficiency variations with angle at Helsinki.

The period consists of 180 days from the winter solstice. The efficiency reaches a peak value of 0.627 at 63 degrees. If the panel is held at 63 degrees then the variation of the efficiency with the days is shown in Figure 7.

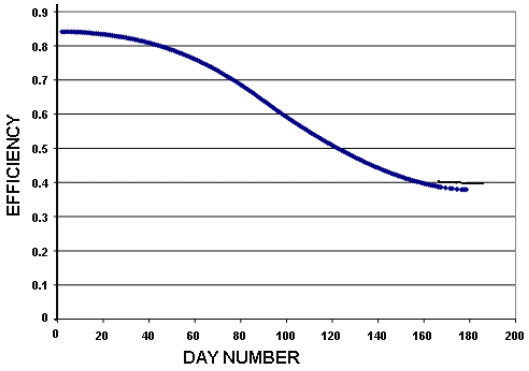

Fig. 7. Efficiency variations with day after winter solstice.

In this figure, one can see that the efficiency decreases with the increase in the number of days after the winter solstice. This is due to the fact that the span of the angular variations in α_s or α has been increasing with the number of days from the winter solstice as explained in Figures 3 and 4 (the curvilinear length increases as days

go by from the winter solstice). One needs to note that - considering $I_0 = 1$, the conversion efficiencies of these stationary solar panels are plotted based on $\{I\}^2$ given in Equation 6. We have to remember that the energy conversion takes place only when $\{I_{X2}\}^2$ is negative. The components $\{I_{Y2}\}^2$ and $\{I_{z2}\}^2$ do not contribute to the energy conversion.

One possible way to further increase the efficiency can be by setting the angle of the panel twice (i.e. fine-tuning of the angle) each for a 90 day span; once between the winter solstice and the spring equinox (period 1) and the other between the spring equinox and the summer solstice (period 2). Since the division into two periods is due to variations of angular spans of α_s and α, the period 1 would need to be extended back to the fall equinox, considering these spans. Likewise, period 2 would include the durations between the summer solstice to the fall equinox.

Figure 8 shows the variation of efficiencies with the angle. It shows two optimums for each of the spans. The value of the peak efficiency for the summer is smaller than that of the winter and the angle at which this peak also occurs is less than that of the winter. Due to the low altitude angle of the sun in the winter, the angle γ in Figure 2 has to be higher to have sunrays incident on it from the normal direction. The variation of efficiency with the number of days after the winter solstice with two settings in place of one is shown in Figure 9.

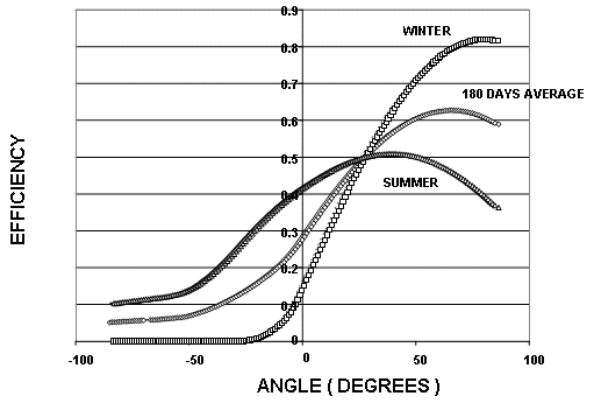

Fig. 8. Efficiency variation with angle at Helsinki with two angle settings.

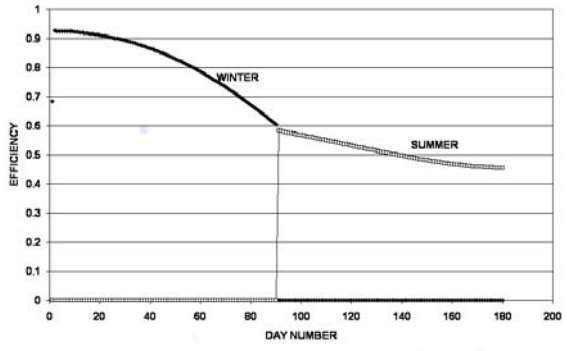

Fig. 9. Efficiency variations with day (angle setting twice).

The average efficiency with these two settings now becomes equal to 0.662 (Figure 9) from 0.627 (Figure 7). Thus, the efficiency is slightly increased by two settings as compared to one setting. If we adopt for a tracking process then this efficiency becomes equal to 1 and this will be a considerable increase. Figures 10 to 15 show the same variations for Singapore which is near the equator.

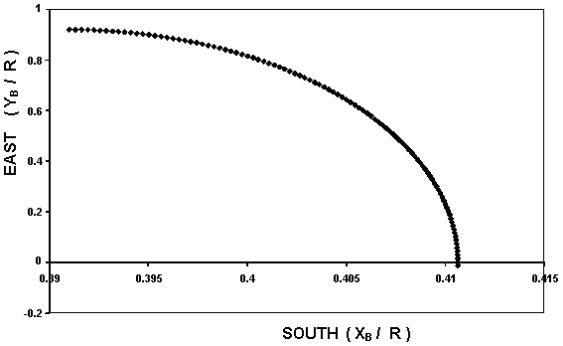

Fig. 10. Solar trajectory at Singapore.

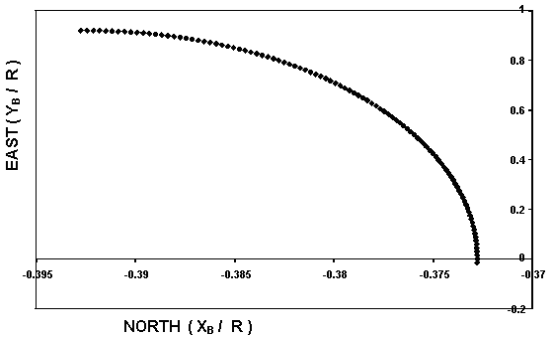

Fig. 11. Solar trajectory at Singapore, N=182.

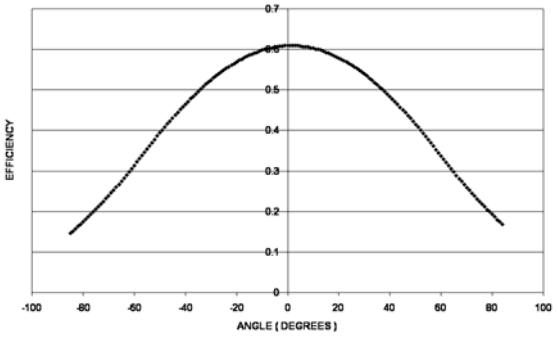

Fig. 12. Efficiency variation with angle at Singapore.

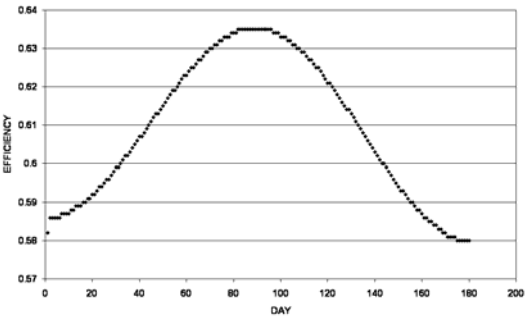

Fig. 13. Efficiency variation with day at Singapore.

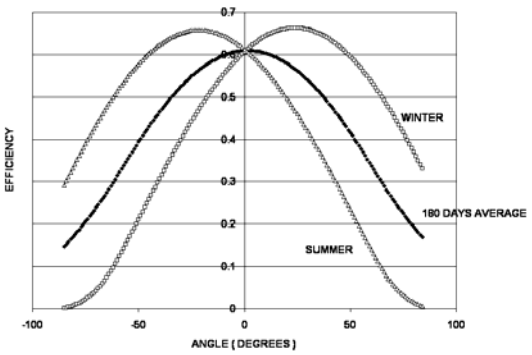

Fig. 14. Efficiency variations with angle at Singapore.

One thing to note in the case of Singapore is that in Figure 14, the angle γ for the summer is negative. This negative value is because the sun stays to the north of the east – west line as shown in Figure 11. The sun never crosses this line as it happened in Figure 4 in the case of Helsinki. In Figure 14, the peak magnitudes for the winter and summer settings are almost equal and each of these is greater than 0.6. The respective variations of the efficiencies are shown in Figure 15. Table 2 shows the summary of results of the four cities situated at different latitudes. It shows that the efficiencies increase from 0.61 to 0.66 more or less, if we go for two settings of the angle γ in all the four cases.

These results are quite comparable to the experimental values (66.667 %) discussed in the Appendix B.

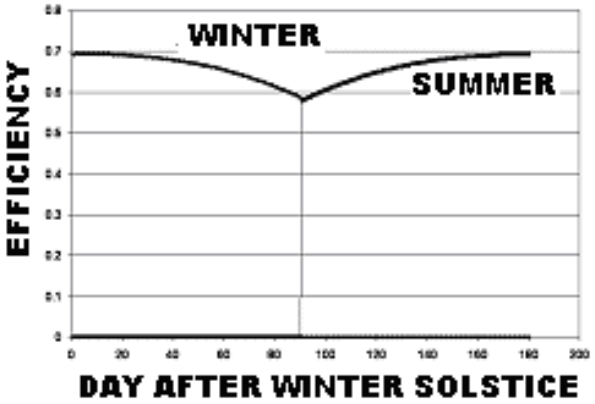

Fig. 15. Variation of efficiency with two settings at Singapore.

Table 2. Efficiencies at four different cities.

City	Latitude (North)	Angle γ (Degrees)	Average Efficiency γ	Angles (γ1, and γ2)	Average Efficiency (γ1, and γ2)
Singapore	1^0 14’	3	0.609	-23, 24	0.660
Patna (India)	25^0 37’	28	0.611	4, 48	0.659
Boulder (USA)	40^0 1’	42	0.614	17, 59	0.659
Helsinki (Finland)	60^0 10’	63	0.624	37, 80	0.662

5. CONCLUSION

In this work, the mathematical equations for the normal incidence on the solar panels were derived first. Thus, based on the studies for 180 days (after the winter solstice) for four cities at varying latitudes, the following conclusions can be drawn:

1. There exists an optimum angle for the panels at various latitudes which yields an efficiency of approximately 0.61.
2. If the angle is set twice in a year, efficiency can be increased to 0.66.
3. The efficiency found between the spring equinox to the summer solstice (the second period) is less than that found between the winter solstice and the spring equinox (the first period).

The decrease in the efficiency in the second period is because of the increased span of the horizontal and vertical angles of the sun’s incident rays.

NOMENCLATURE

[R (Y1, η)]	Rotation matrix to transform
$\{I\}^1$	The intensity vector in X1 –Y1 – Z1 co-ordinate frame
$\{I\}^2$	The intensity vector in X2 –Y2 – Z2 co-ordinate frame
α	Angle in vertical plane
α_s	Angle in horizontal plane
γ	Latitude of the place
δ	Declination
θ_1	Angle of incidence
θ_2	Angle of refraction
h_s	Hour angle at any instant of time
h_{sr}	Hour angle at sunrise measured from noon
I_0	Incident solar energy intensity of beam radiation
A	Absorptance
r	Reflectance
N	Day number of a year
R	Distance from the earth to sun
T	Transmittance
X_B / R	Normalized x co-ordinate of the projection of the sun on the horizontal plane shown as point B in Fig. 1.
Y_B / R	Normalized y co-ordinate of the projection of the sun on the horizontal plane shown as point B in Fig. 1.

REFERENCES

[1] Bentley, R.W. 2004. Global oil depletion–methodologies and results. In *Proceedings of the 3rd International Workshop on Oil and Gas Depletion*, Berlin, Germany, May 25-26.

[2] Luque, A., Cuevas, A., and Ruiz, L.M. 1980. Double-sided n^+-p-n^+ solar cell for bifacial concentration. *Sol Cells* 2: 151-166.

[3] Luque, A., Lorenzo, E., and Sala, G. 1984. Diffusing reflectors for bifacial photovoltaic panels. *Sol. Cells.* 13: 277-292.

[4] Forrest, S.R., and Xue, J. 2005. Strategies for solar energy power conversion using thin film organic photovoltaic cells. In *Proceedings of 31st IEEE Photovoltaic Specialists Conference*, 3-7 January: 23-26.

[5] Vorobiev, Y., Gonzalez-Hernandez, J., Vorobiev, P., and Bulat, L. 2004. Thermal-photovoltaic solar hybrid system for efficient solar energy conversion, *Solar Cells and Solar Energy Materials*, 170-176.

[6] Hiyama, T. Kouzumu, S., and Imakubo, T. 1995. Evaluation of neural network based real time maximum power tracking controller for PV systems. *IEEE Transactions on Energy Conversion* 10: 543-548.

[7] Husain, K.H., Muta, I., and Hoshino, T. 1995. Maximum photoelectric power tracking: an algorithm for rapidly changing atmospheric conditions. *IEEE Proceedings, Generation, Transmission, and Distribution* 142: 59-64.

[8] Huynh, P.T., and Cho, B.H, 1999. Design and analysis of a regulated peak-power tracking system. *IEEE Transactions on Aerospace and Electronic Systems* 35(1): 84-92.

[9] Huynh, P., and Cho, B.H., 1996. Design and analysis of a microprocessor-controlled peak-power tracking system. *IEEE Transactions on Aerospace and Electronic Systems* 32: 182-190.

[10] Baz A., Sabry A., and Mobarak, A.1984. On the tracking error of a self-contained solar tracking system. *Journal of Solar Energy Journal, Transactions. ASME* 106: 416-422.

[11] Farber, K., Morrison, C.A., and Ingely, H.A. 1976. A self-contained tracking system. *ASME* Paper No. 76 - WA/HT - 26, December.

[12] Hiyama, T., Shinichi K., and Tomofumi, I. 1994. Identification of optimal operating point of PV modules using neural network for real time maximum power tracking control. *IEEE Transactions on Energy Conversion* 10(2): 360-367.

[13] Maish, A.B. 1990. Performance of a self aligning solar array tracking controller. In *21st IEEE Photovoltaic Conference*, pp. 864-869. Kissimimee, Florida, USA.

[14] Ro, K., and Rahman, S., 1998. Two-loop controller for maximizing performance of a grid-connected photo-voltaic cell hybrid power plant. *IEEE Transactions on Energy Conversion* 13(3): 276–281.

[15] Siri, K., Caliskan, V.A., and Lee, C.Q. 1993. Peak power tracking in parallel connected converters. *IEEE Proceedings, Part G, Circuits, Devices, and Systems* 140: 106–116.

[16] Mellit, A., Benghanem, M., Bendekhis, M., 2005. Artificial neural network model for prediction solar radiation data: application for sizing stand-alone photovoltaic power system. *IEEE Power Engineering Society General Meeting* 1: 40-44.

[17] Bird, R.E., and Riordan, C. 1986. Simple solar spectral model for direct and diffuse irradiance. Journal of Applied Meteorology 25: 87-97.

[18] Iskender, I. 2005. A fuzzy logic controlled power electronic system for maximum power point detection of a solar energy panel. *The International Journal for Computation and Mathematics in Electrical and Electronic Engineering* 24(4): 1164-1179.

[19] Klutcher, T.M. 1979. Evaluating model to predict insolation on tilted surfaces. *Solar Energy* 23: 111-123.

[20] Satyamurty, V.V., and Labiri, P.K. 1992. Estimation of symmetric and asymmetric hourly global and diffuse radiation from daily values. *Solar Energy* 48: 7-14.

[21] Sen, Z. 1998. Fuzzy algorithm for estimation of solar irradiation from sunshine duration. *Solar Energy* 68: 39-49.

[22] Yu, V.P., Gonzalez-Hernandez, J., and Vorobiev, Y.V. 2004. Optimization of the solar energy collection in tracking and non-tracking photovoltaic solar system. In *1st International Conference on Electrical and Electronics Engineering (ICEEE)*, 24-27 June: 310-314.

[23] Exell, R.H.B. 1986. A program in BASIC for calculating solar radiation in tropical climates on small computers. *Renewable Energy Review Journal* 8(2): 11.

[24] Craig, J.J. 2005. *Introduction to Robotics, Mechanics and Control*. Pearson Prentice Hall, New Jersey, USA. Chapter 2.

[25] Kreider, J.F., and Kreith, F. 1979. *Solar Engineering Handbook*. McGraw Hill Book Company, USA. Chapters. 1 and 2.

[26] Kreith, F., and Black, W.Z. 1980. *Basic Heat Transfer*, Harper and Row Publishers, New York, USA. Chapter 6.

[27] Duffie, J.A., and Beckman, W.A. 1991. *Solar Engineering of Thermal Processes, 2nd Edition.* Wiley- Interscience, New York, USA. Chapters 1, 2 and 4.

[28] Garg, H.P. 1982. *Treatise in Solar Engineering: Volume 1 - Fundamentals of Solar Energy.* John Wiley & Sons, Chapter 4.

APPENDIX A

Figure 16 shows a ray of light incident on a glass surface.

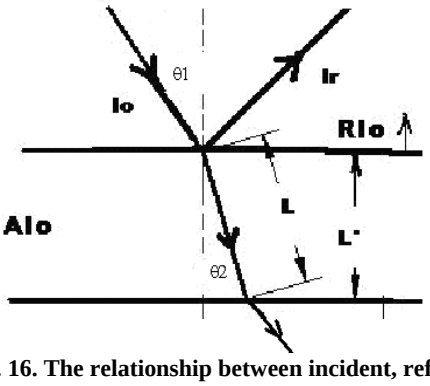

Fig. 16. The relationship between incident, reflected, transmitted, and absorbed solar energy.

A part of the incident energy is reflected, and a part absorbed by the glass. The equation governing reflected fraction r, and transmitted T are given by [28].

$$r = \frac{0.5000000000\sin(\theta 1 - \theta 2)^2}{\tan(\theta 1 + \theta 2)^2} + \frac{0.5000000000\tan(\theta 1 - \theta 2)^2}{\tan(\theta 1 + \theta 2)^2} \quad \text{(A-1)}$$

$$T = (1 - r)/(1 + r) \quad \text{(A-2)}$$

Figure 17 shows a plot of percentage of the incident energy that is reflected. It is a very small fraction whereas, the transmitted fraction is quite large. The losses are very small fractions unless the angle increases beyond 64 degrees. The absorptance A in glass is given by:

$$A=\exp(-KL) \quad \text{(A-3)}$$

Here, K is the absorptivity and L is the path length which is shown in the Figure 16. The value of K for glass containing 0.02% ferrous oxide is approximately equal to 0.04 per centimeter path length.

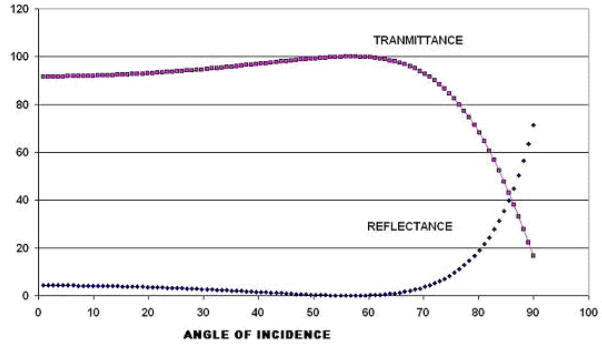

Fig. 17. Plot of reflectance and transmittance.

APPENDIX B

The theoretical derivations carried out in this work, match well with those obtained through experiments. The experiments were carried out at St. John's, Canada. In the static readings, the panel was facing south (static) at an angle from horizontal equal to the latitude of St. John's (47^{0} 37' N), and in the other set - (by tracking the sun), the correct tracking was checked where the pointer did not have any shadows during the tracking. The DC Power was calculated by measuring the voltage and the current at different instants of time of the day. The result obtained is shown in Figure 18.

A polynomial was fitted through the experimental points as shown in the figure. The areas under each of the two curves were obtained. In the case of the polynomial curve, it was integrated. The efficiency was calculated by finding the ratio of the areas. The ratio came out to be equal to 66.667% which is close to the theoretically obtained values. The numerical values of the static readings are shown in Table 3. In Figure 18, the tracking values are equal to the maximum of the static values occurring at noon.

Figure 19 shows the solar tracking system which is rotated at the rate of the spin of the earth but in opposite direction. The axis of rotation is parallel to the spin axis of the earth. It also has an axis (horizontal) to change the declination (the inner frame is rotated about the outer frame about an axis which is orthogonal to the rotation axis). Therefore, this machine can be used for static results also by orienting the panel towards the south and holding the shaft stationary.

Table 3. The static results.

Number	Time (min)	Current (A)	Voltage (V)	Power (W)
1	71.8	3.3	12.9	42.3
2	83.9	3.3	12.9	42.6
3	99.0	3.2	12.9	41.3
4	111.0	3.2	12.9	41.3
5	120.1	3.1	12.9	40.0
6	129.8	2.2	12.7	27.9
7	142.7	2.8	12.8	35.8
8	155.7	1.4	12.5	17.5
9	179.6	0.8	12.3	9.8

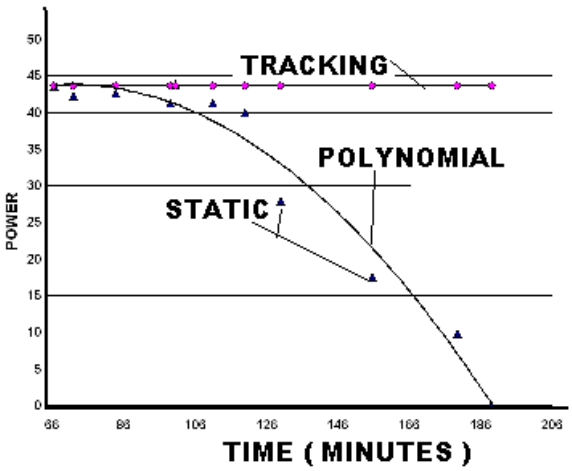

Fig. 18. DC power versus time.

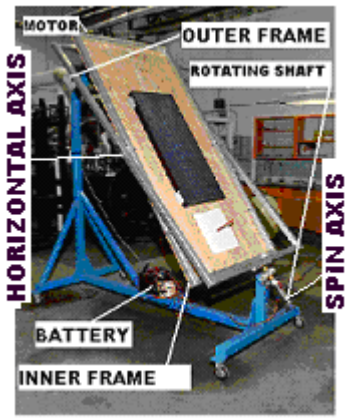

Fig. 19. The solar tracking system.